



OPEN

SLC7A11, a potential immunotherapeutic target in lung adenocarcinoma

Qingqing Shan, Chi Zhang, Yangke Li✉, Qunying Li✉, Yifan Zhang, Xue Li, Junqing Shi & Fengying Hu

SLC7A11 has significant translational value in cancer treatment. However, there are few studies on whether *SLC7A11* affects the immune status of lung adenocarcinoma (LUAD). Information on *SLC7A11* expression and its impact on prognosis was obtained from the cancer genome atlas and gene expression omnibus databases. The differentially expressed genes (DEGs) were analysed by GO and KEGG. GSEA enrichment analysis was performed in the *SLC7A11*-high and *SLC7A11*-low groups. The relationship between *SLC7A11* and tumour immunity, immune checkpoints, and immune cell infiltration was studied using R language. We analysed the correlation between *SLC7A11* and chemotactic factors (CFs) and chemokine receptors using the TISIDB database. *SLC7A11* is overexpressed in many tumours, including LUAD. The 5-year overall survival of patients in the *SLC7A11*-high group was lower than in the *SLC7A11*-low group. KEGG analysis found that the DEGs were enriched in ferroptosis signaling pathways. GSEA analysis found that the survival-related signaling pathways were enriched in the *SLC7A11*-low group. The *SLC7A11*-low group had higher immune scores and immune checkpoint expression. *SLC7A11* was negatively correlated with many immune cells (CD8+T cells, immature dendritic cells), CFs, chemokine receptors (such as CCL17/19/22/23, CXCL9/10/11/14, CCR4/6, CX3CR1, CXCR3) and MHCs (major histocompatibility complex). *SLC7A11* may regulate tumour immunity and could be a potential therapeutic target for LUAD.

Abbreviations

BP	Biological process
BRCA	Breast cancer
CC	Cellular component
<i>CCL</i>	C–C motif chemokine ligand
<i>CCR</i>	C–C motif chemokine receptor
CFs	Chemotactic factors
CHOL	Cholangio carcinoma
COAD	Colon adenocarcinoma
<i>CTLA4</i>	Cytotoxic T-Lymphocyte associated Antigen 4
<i>CX3CR</i>	C-X3-C motif chemokine receptor
<i>CXCL</i>	C-X-C motif chemokine ligand
DEGs	Differentially expressed genes
GEO	Gene expression omnibus
GO	Gene ontology
GSEA	Gene set enrichment analysis
GSH	Glutathione
HNSC	Head and neck squamous cell carcinoma
KEGG	Kyoto encyclopedia of genes and genomes
KIRC	Kidney renal clear cell carcinoma
KIRP	Kidney renal papillary cell carcinoma
<i>LAG3</i>	Lymphocyte activating 3

Department of Respiration, Chengdu First People's Hospital, No. 18, Wangxiang North Road, High-Tech Zone, Chengdu 610041, Sichuan Province, People's Republic of China. ✉email: yangkeli1978@sina.com; qunyingli1963@126.com

LIHC	Liver hepatocellular carcinoma
LUAD	Lung adenocarcinoma
LUSC	Lung squamous cell carcinoma
MDSC	Myeloid-derived suppressor cells
MF	Molecular function
MHC	Major histocompatibility complex
MHCs	Major histocompatibility complex
NSCLC	Non-small cell lung cancer
OS	Overall survival
<i>PD-L1</i>	Programmed death ligand 1
PRAD	Prostate adenocarcinoma
READ	Rectum adenocarcinoma
ROS	Reactive oxygen species
<i>SLC7A11</i>	Solute carrier family 7 member 11
STAD	Stomach adenocarcinoma
TCGA	The cancer genome atlas
<i>TGF-β1</i>	Transforming growth factor β 1
Treg	Regulatory T cell
x_c^-	The cystine/glutamate transporter system
UCEC	Uterine corpus endometrial carcinoma

In recent years, with the accelerated development of targeted therapy and immunotherapy, the mortality rate of lung cancer has dramatically decreased. However, lung cancer remains the leading cause of cancer death in men and women over 50 years old¹. Tumour resistance and immune escape limit the therapeutic effects in patients with advanced adenocarcinoma². Therefore, finding new targets to prevent or slow disease progression is a priority.

SLC7A11 and *SLC3A2* encode the cystine/glutamate transporter system (system x_c^-), which transports cysteine into cells in exchange for glutamate³. Both cysteine and glutamate are important endogenous substances. Cysteine is an important part of the redox system, playing a crucial role in balancing reactive oxygen species (ROS). ROS and ROS-mediated signaling pathways are involved in various cellular and biochemical processes, including cell apoptosis, ferroptosis, autophagy, cell proliferation and migration, endoplasmic reticulum stress, mitochondrial dysfunction, DNA damage, cell metabolism, and drug resistance⁴. Recent studies have found that *SLC7A11* may be an independent prognostic factor for LUAD⁵. However, whether *SLC7A11* can be an effective target for LUAD treatment requires more theoretical support.

In this study, we analysed the expression of *SLC7A11* and clinical information in LUAD patients. Then, we used GO/KEGG and GSEA for enrichment analysis. We analysed the correlation between *SLC7A11* and immune cells, checkpoint expression, and CFs.

The results showed that *SLC7A11* overexpression was negatively correlated with CFs in the immune micro-environment. Reduction of CFs might reduce immune cell infiltration, leading to immunosuppression and immune escape and thus protecting tumour cells from immune cell attack. Targeted inhibition of *SLC7A11* may enhance the tumour immune response.

Materials and methods

Data source

The TCGA database (<https://portal.gdc.cancer.gov/>) is an accessible data portal for collecting information related to cancer patients.

The TCGA database includes 54 normal samples and 497 LUAD samples. After removing samples with incomplete survival data and duplicates, a total of 468 LUAD samples with RNA-Seq expression and matched clinical information (including pathological staging, OS time, gender, and age) were obtained. The RNA-Seq expression data of a pan-cancer analysis were also obtained from the TCGA database. The GSE30219, GSE37745, and GSE68465 datasets were obtained from the GEO database (<https://www.ncbi.nlm.nih.gov/geo/>), and detailed information is shown in Table 1.

DEGs analysis

We analysed differences in the expression of *SLC7A11* between normal and LUAD samples in the TCGA-LUAD, GSE30219, GSE37745, and GSE68465 datasets. We divided TCGA-LUAD samples into an *SLC7A11*-high group and *SLC7A11*-low group based on the mean expression value of *SLC7A11*. The DEGs between the

Dataset	Platform	Submission date	Last update date	Country	Control	LUAD
GSE30219	GPL570	40,720	43,549	France	14	85
GSE37745	GPL570	41,032	44,707	Sweden	0	106
GSE68465	GPL96	42,125	43,322	USA	19	443

Table 1. The detailed information of three data sets in the GEO database.

SLC7A11-high and *SLC7A11*-low group were identified using the “limma” R package⁶ and a total of 622 DEGs were obtained (criteria: $|\log_{2}FC| > 2$ and $adj.P.val < 0.05$).

Survival analysis

The “survival” and “survminer” R packages were used to perform survival analysis in the *SLC7A11*-high and *SLC7A11*-low groups in the TCGA-LUAD dataset. We validated the survival analysis results in the GSE68465 dataset.

We also performed a survival analysis in the KM Plotter database (<https://kmplot.com/analysis/>). In the lung cancer analysis interface, we selected “adenocarcinoma” as the “histology,” “OS” for “survival,” “60 months” as the “follow-up threshold,” “*SLC7A11*” as the “gene symbol,” and “auto selected best cutoff” for “split patients by”. A total of 1161 LUAD samples were analysed for survival. In the pan-cancer analysis interface, 7462 pan-cancer samples were analysed for survival, and detailed information on the pan-cancer samples is shown in Table 2.

Gene enrichment analysis

GO analysis includes three parts: molecular function (MF), biological process (BP), and cellular component (CC)⁷. The KEGG pathway database is currently the most widely used public database of metabolic pathways⁸. We used the Database for Annotation, Visualization and Integrated Discovery (DAVID) (<https://david.ncifcrf.gov/tools.jsp>) to perform GO and KEGG analysis on the 622 DGEs.

GSAE analysis was performed using “c2.cp.kegg.v7.4.symbols.gmt” as the reference genome in R language⁹.

The relationship between *SLC7A11* and tumour immunity

In the TCGA-LUAD dataset, the “commonGenes.gct” and “estimateScore.gct” files were read in R language, and the “estimate” was used to score the immune score, stromal score, and immune cell infiltration for each tumour sample¹⁰. We compared the immune and stromal scores between the *SLC7A11*-high and *SLC7A11*-low group using the “limma” package, and analysed the correlation between *SLC7A11* and immune cell infiltration and common immune checkpoints using the “corrplot” package. The correlation between *SLC7A11* and *SLC3A2* was analyzed by the Sangbox 3.0 (<http://sangerbox.com/home.html>).

We validated the correlation between *SLC7A11* and immune cell infiltration in the GSE30219, GSE37745, and GSE68465 datasets.

Relationship between *SLC7A11* and CFs

We evaluated the correlation between *SLC7A11* and CFs, chemokine receptors, and MHCs in the tumour micro-environment using the “chemokines” module of the TISIDB database (<http://cis.hku.hk/TISIDB/>).

Screening of potential therapeutic drugs

We then used the “pRRophetic” R package to assess the treatment response, as indicated by the IC_{50} of targeted and immunotherapy drugs¹¹.

Cancer	Number	<i>p</i>
Bladder carcinoma	405	0.036
Breast cancer	1090	0.0109
Cervical squamous cell carcinoma	304	0.0085
Esophageal adenocarcinoma	80	0.079
Esophageal squamous cell carcinoma	81	0.11
Head-neck squamous cell carcinoma	500	0.0037
Kidney renal clear cell carcinoma	530	0.00058
Kidney renal papillary cell carcinoma	288	4.9e-10
Liver hepatocellular carcinoma	371	8.2e-8
Lung adenocarcinoma	513	0.0042
Ovarian cancer	374	0.00055
Pancreatic ductal adenocarcinoma	177	0.01
Pheochromocytoma and Paraganglioma	178	0.067
Rectum adenocarcinoma	165	0.0062
Sarcoma	259	0.011
Stomach adenocarcinoma	375	0.071
Testicular germ cell tumor	134	0.13
Thymoma	119	0.026
Thyroid carcinoma	502	0.062
Uterine corpus endometrial carcinoma	543	0.0043

Table 2. The detailed information of pan-cancer survival analysis in KM-plot.

Result

Overexpression of *SLC7A11* in LUAD

In the pan-cancer analysis, *SLC7A11* was found to be overexpressed in tumours such as breast cancer (BRCA), cholangiocarcinoma (CHOL), colon adenocarcinoma (COAD), head and neck squamous cell carcinoma (HNSC), kidney renal clear cell carcinoma (KIRC), kidney renal papillary cell carcinoma (KIRP), liver hepatocellular carcinoma (LIHC), lung squamous cell carcinoma (LUSC), LUAD, prostate adenocarcinoma (PRAD), rectum adenocarcinoma (READ), stomach adenocarcinoma (STAD), and uterine corpus endometrial carcinoma (UCEC) (Fig. 1A).

In the GSE30219 and GSE68465 datasets, the expression of *SLC7A11* was higher in LUAD than in normal tissues ($p < 0.05$) (Fig. 1B,C).

The TCGA-LUAD dataset showed no significant difference in *SLC7A11* expression among ages or stages (Fig. 1D,E).

Relationship between *SLC7A11* and prognosis in LUAD

Survival analysis of the TCGA-LUAD dataset showed that the 5-year OS of the *SLC7A11*-high group was lower than that of the *SLC7A11*-low group ($p < 0.05$) (Fig. 2A). In the GSE68465 dataset the *SLC7A11*-low group had a longer 5-year OS than the *SLC7A11*-high group. ($p < 0.05$) (Fig. 2B). The expression of *SLC7A11* was higher in deceased patients than in surviving patients (Fig. 2C).

In the Kaplan–Meier Plotter database, the *SLC7A11*-low group showed a longer 5-year OS than the *SLC7A11*-high group ($p < 0.05$) (Fig. 2D). The pan-cancer analysis showed that the 5-year OS of the *SLC7A11*-high group was lower than that of the *SLC7A11*-low group for many tumours ($p < 0.05$) (Fig. 2E and Table 2).

DEGs analysis and GO/KEGG analysis

The TCGA-LUAD database contained 622 DEGs between the *SLC7A11*-high and *SLC7A11*-low groups (Fig. 2F).

GO-MF analysis showed that DEGs are mainly enriched in molecular function pathways such as protein binding, cadherin binding, identical protein binding, and enzyme binding (Fig. 3A).

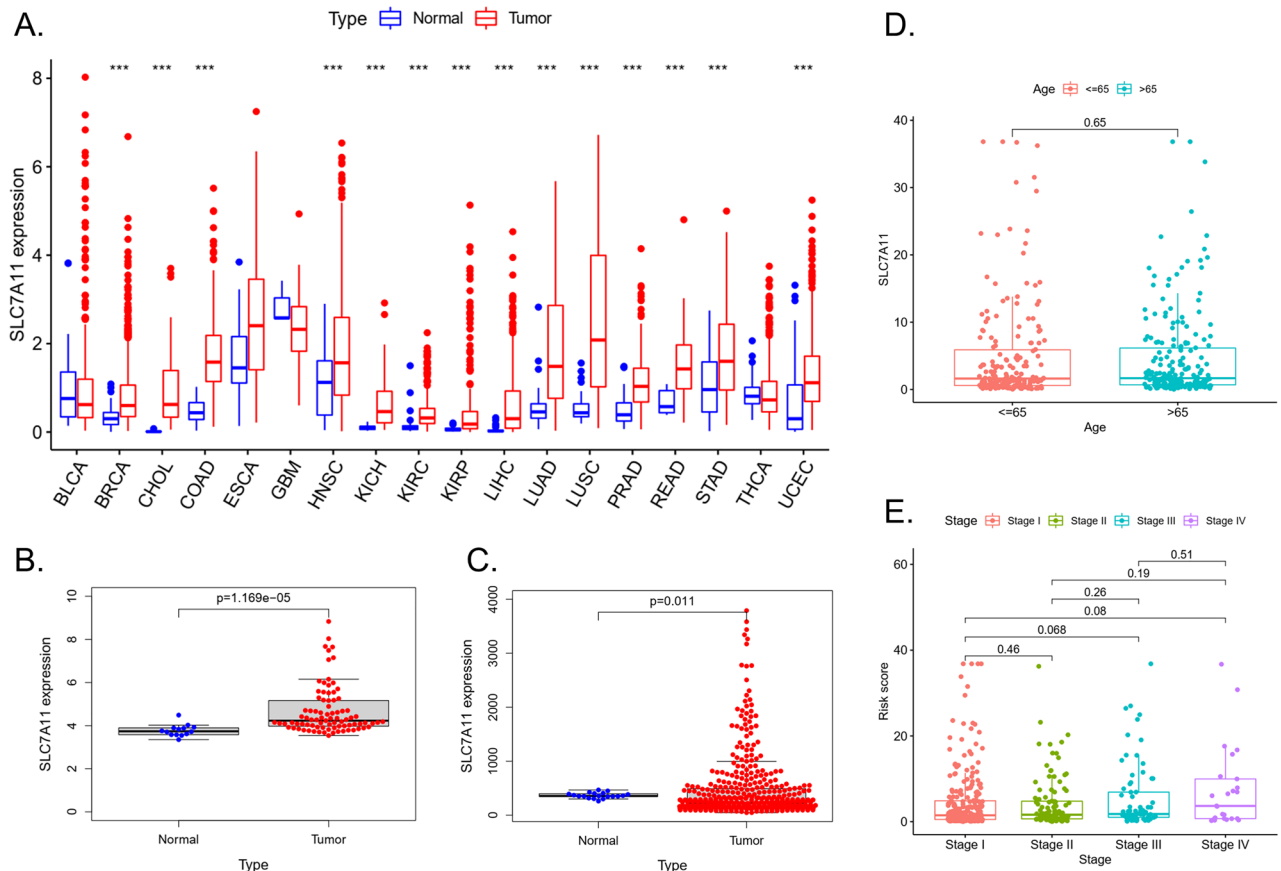


Figure 1. The expression of *SLC7A11* in the tumor. (A) *SLC7A11* expression in distinct cancers compared with normal tissues in TCGA. (B) *SLC7A11* expression LUAD compared with normal tissues in the GSE30219 database. (C) *SLC7A11* expression LUAD compared with normal tissues in the GSE68465 database. (D) *SLC7A11* expression of different ages in LUAD patients. E. *SLC7A11* expression of different stages in LUAD patients.

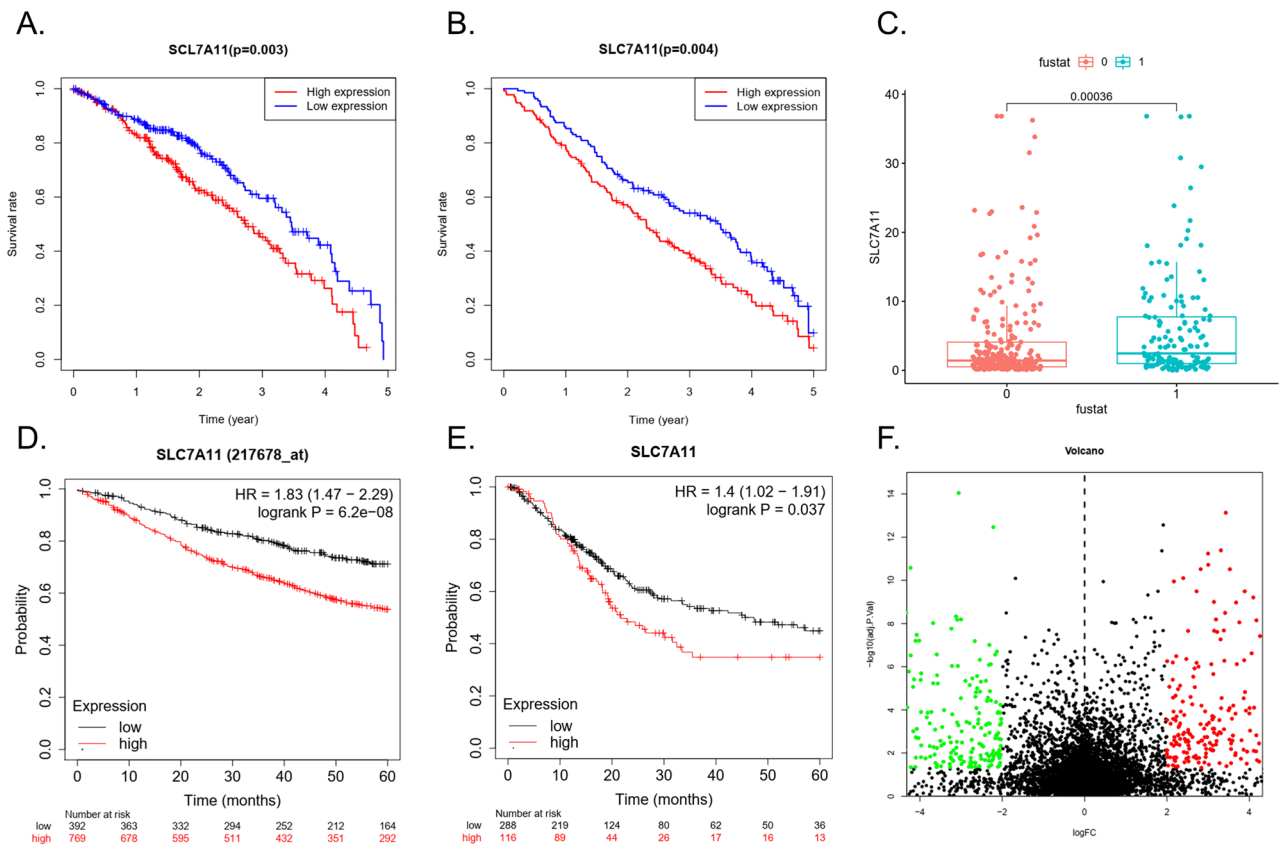


Figure 2. Survival analysis. (A) 5-year OS of the *SLC7A11*-high group and *SLC7A11*-low group in TCGA-LUAD dataset. (B) 5-year OS of the *SLC7A11*-high group and *SLC7A11*-low group in the GSE68465 dataset. (C) The expression of *SLC7A11* in LUAD with different survival states in the TCGA-LUAD dataset. Survival curve of LUAD in KM-plot. Survival curve of pan-cancer in KM-plot (Bladder Carcinoma). (F) DEGs in the *SLC7A11*-high group and *SLC7A11*-low group.

GO-BP analysis showed that the DEGs were mainly enriched in the defense response to Gram-positive bacteria, the negative regulation of cAMP-mediated signaling, and apoptosis-related biological processes. More details are shown in Fig. 3B.

GO-CC analysis showed that DEGs were mainly enriched in cellular components such as extracellular exosomes, endoplasmic reticulum, membranes, extracellular spaces, and cytosol (Fig. 3C).

KEGG enrichment analysis found that DEGs were mainly enriched in pathways such as osteoclast differentiation, ferroptosis, viral myocarditis, arachidonic acid metabolism, and viral carcinogenesis, among which four pathways were related to immunity, three pathways were related to metabolism, and one pathway was related to ferroptosis (Fig. 3D).

GSEA analysis revealed that in the *SLC7A11*-high group, gene sets were mainly enriched in metabolism-related signaling pathways, such as steroid hormone biosynthesis, metabolism of xenobiotics by cytochrome p450, ascorbate and aldarate metabolism, histidine metabolism, and tyrosine metabolism (Fig. 3E).

In the *SLC7A11*-low group, gene sets were mainly enriched in immune-related signaling pathways, such as viral myocarditis, the intestinal immune network for IgA production, asthma, and allograft rejection (Fig. 3F).

The relationship between *SLC7A11* and tumour immunity

KEGG and GSEA analysis showed differences in immune-related signaling pathways between the *SLC7A11*-high group and *SLC7A11*-low group. Therefore, we also analysed the immune status of the two groups.

In the TCGA-LUAD dataset, the immune (Fig. 4A), stromal (Fig. 4B), and ESTIMATE (Fig. 4C) scores of the *SLC7A11*-high group were lower than those of the *SLC7A11*-low group. *SLC7A11* expression was negatively correlated with many immune checkpoints, such as *BTLA*, *CD244*, *CD247*, *CD40*, *CTLA4*, and *ICOS* (Fig. 4D).

SLC7A11 expression was negatively correlated with T cells, B lineage, and myeloid dendritic cells, but positively correlated with neutrophils (Fig. 4E). In the GSE37745, GSE68465, and GSE68465 datasets, the expression of *SLC7A11* was negatively correlated with many immune cells, such as central memory CD8 T cells, effector memory CD8 T cells, immature dendritic cells, and type 1 T helper cells. In the GSE68465 dataset, *SLC7A11* was also positively correlated with neutrophils (Fig. 5A,B,C).

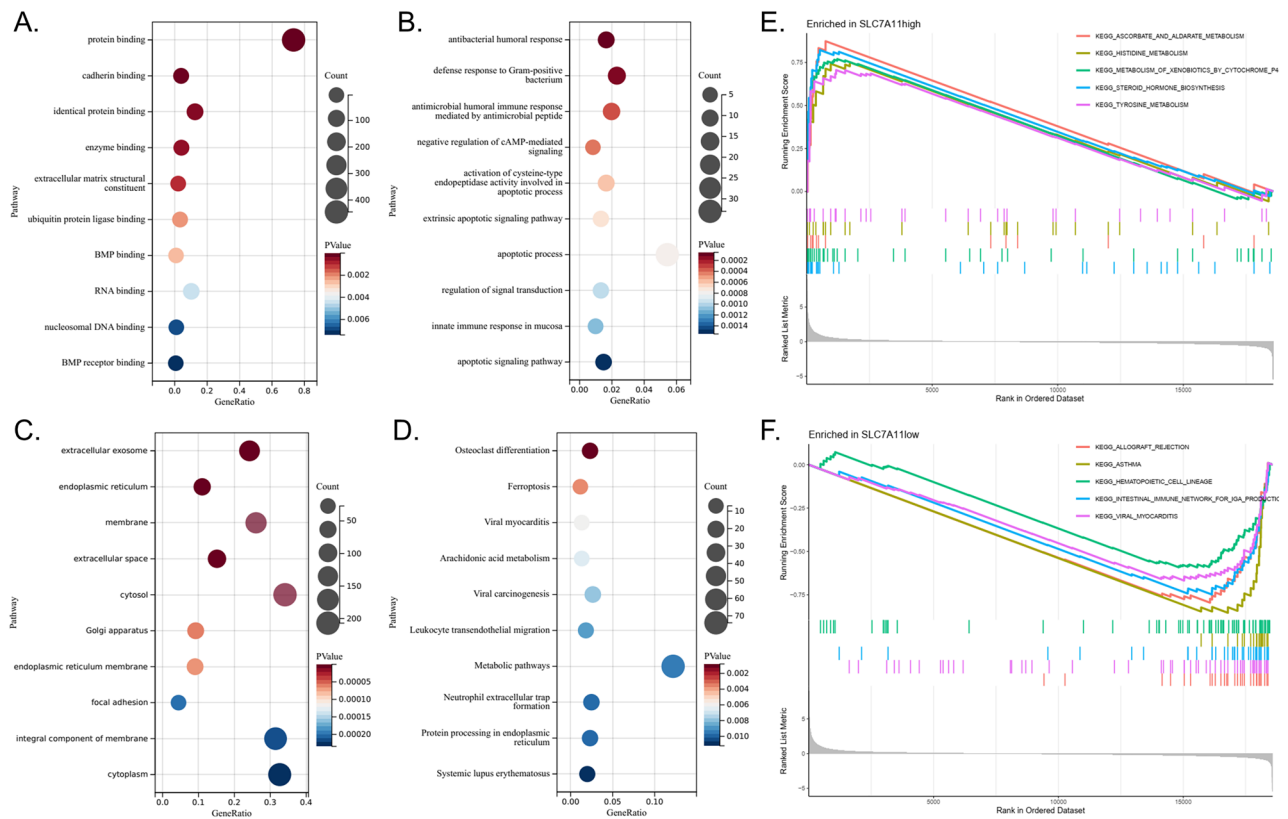


Figure 3. Enrichment analysis. **(A)** GO-MF analysis of DEGs in LUAD. **(B)** GO-BP analysis of DEGs in LUAD. **(C)** GO-CC analysis of DEGs in LUAD. **(D)** GO-KEGG analysis of DEGs in LUAD. **(E)** GSEA analysis in the *SLC7A11*-high group. **(F)** GSEA analysis in the *SLC7A11*-low group.

Relationship between *SLC7A11* and CFs

The role of CFs in tumour immunity is related to tumour immune escape. *SLC7A11* expression was negatively correlated with most CFs (Table 3), chemokine receptors (Table 4), and MHCs (Table 5).

Relationship between *SLC7A11* and *SLC3A2*

In the TCGA-LUAD dataset, the expression of *SLC7A11* showed a significant correlation with that of *SLC3A2* ($p < 0.05$) (Fig. 5D), a known partner for *SLC7A11*. In the TCGA-LUAD dataset, the immune (Supplement Fig. 1A), stromal (Supplement Fig. 1B), and ESTIMATE (Supplement Fig. 1C) scores of the *SLC3A2*-high group were lower than those of the *SLC3A2*-low group.

Drug sensitivity analysis

We identified 10 immunotherapeutic or targeted agents that showed lower IC_{50} values in the *SLC7A11*-high group than in the *SLC7A11*-low group, including two insulin-like growth factor 1 receptor/insulin receptor inhibitors, two HSP90 ATPase inhibitors, and two tyrosine, serine/threonine kinase inhibitors (Fig. 6A,B,C,D). We also identified 20 drugs with low IC_{50} values in the *SLC7A11*-low group (Fig. 6E,F,G,H).

Discussion

With the development of early detection, surgical treatment, precise pathological staging, targeted therapy and immunotherapy, the survival rate of lung cancer has improved. The 3-year OS for lung cancer increased from 22% in 2004–2006 to 33% in 2016–2018. However, lung cancer remains the leading cause of cancer death in men and women aged 50 and over¹. Among all lung cancers, LUAD accounts for about 50% of cases.

This study found that *SLC7A11* is highly expressed in cancers such as breast cancer, LUSC, LUAD, and gastric cancer. In addition, patients with high *SLC7A11* expression had a lower 5-year OS than those with low *SLC7A11* expression.

Treatment failure in LUAD is related to many factors, such as tumour heterogeneity, immune escape, and chemotherapy resistance¹². Most studies suggest that *SLC7A11* overexpression is related to immune escape. The current study found that high *SLC7A11* expression is associated with treatment failure in immune therapy, indicating that *SLC7A11* is associated with the efficacy of immune therapy. This is because high *SLC7A11* expression can increase the concentration of specific metabolites in tumour cells, such as GSH, which inhibits the activation of immune cells and the apoptosis of tumour cells, thereby reducing the efficacy of immune therapy¹³. Some studies have shown that *SLC7A11* can affect tumour immune escape and the anti-tumour immune response by regulating intracellular redox balance and tumour cell metabolism and growth. Inhibiting *SLC7A11* can enhance

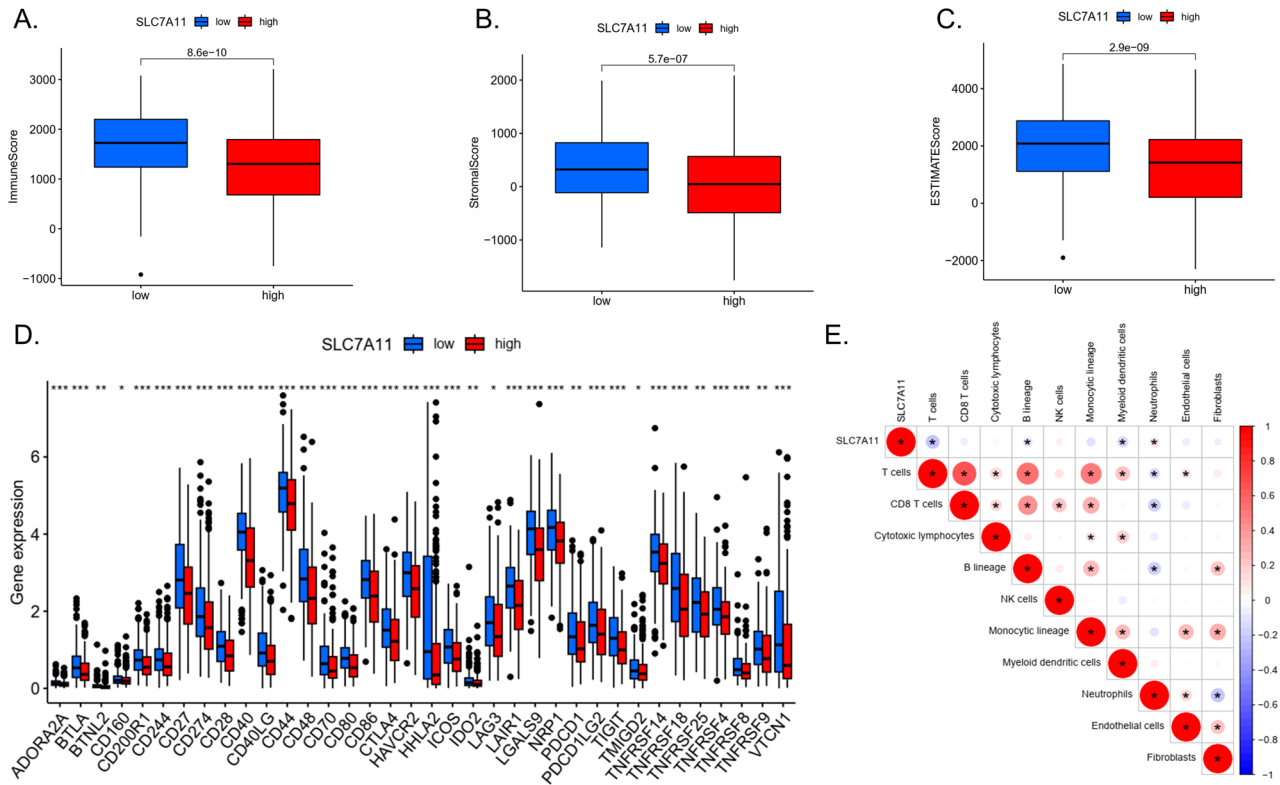


Figure 4. Immune analysis. (A) Immune cells score in the *SLC7A11*-high group and *SLC7A11*-low group. (B) Stromal cells score in the *SLC7A11*-high group and *SLC7A11*-low group. (C) ESTIMATE scores in the *SLC7A11*-high group and *SLC7A11*-low group. (D) The difference of 29 immune checkpoints expression in the *SLC7A11*-high group and *SLC7A11*-low group. (E) The correlation between *SLC7A11* expression and immune cells in the TCGA-LUAD database. (***) $p < 0.001$; (**) $p < 0.01$; (*) $p < 0.05$.

the attack of tumour cells by immune cells and improve the efficacy of immune therapy¹⁴. However, blocking the expression of *SLC7A11* does not affect the normal development of mouse embryos¹⁵. Therefore, drugs that block *SLC7A11* may be ideal anticancer drugs.

Ferroptosis is a newly discovered type new type of cell death caused by the excessive accumulation of iron ions in cells. It was found that *SLC7A11* plays an essential protective role in ferroptosis. Ferroptosis may exert antitumour effects by boosting the immune response and killing cancer cells, and it also has a direct impact on immune cells¹⁶. KEGG analysis found that the DEGs were enriched in the ferroptosis signaling pathway.

In this study, we found that as well as a lower immune score, matrix score, and ESTIMATE score in the *SLC7A11*-high group, expression of the immune checkpoint, including *CD274* (*PD-L1*), *CTLA4*, and *LAG3*, was also lower. GSEA analysis showed that signaling pathways related to metabolism were enriched in the *SLC7A11*-high group, while signaling pathways related to immunity were enriched in the *SLC7A11*-low group. In TCGA-LUAD, *SLC7A11* was negatively correlated with the expression of T cells, B lymphocytes, and myeloid cells and positively correlated with the expression of neutrophils.

A high proportion of neutrophils can inhibit the function of immune cells such as CD8+ T cells and promote tumour growth¹⁷. In the GEO dataset, the expression of *SLC7A11* was negatively correlated with the central memory CD8 T cells, effector memory CD8 T cells, immature dendritic cells, and type 1 T helper cells, all of which play an important role in killing tumour cells. In the GSE68465 dataset, we also observed a positive correlation between *SLC7A11* and neutrophils, which is consistent with TCGA-LUAD.

Interestingly, the expression of *SLC7A11* was negatively correlated with the expression of Treg (regulatory T cell) and MDSC (myeloid-derived suppressor cells). Treg cells and MDSC play an important role in the immune escape of tumour cells in the tumour microenvironment¹⁸. Therefore, the impact of *SLC7A11* on tumour immune cells may be very complex.

Activated CD8+ T cells release IFN- γ and then activate the JAK-STAT1 pathway, resulting in the translocation of phosphorylated STAT1 to the nucleus, thus inhibiting the transcription of *SLC7A11*^{19,20,21,22,23}. In addition, *TGF- β 1* (transforming growth factor β 1) released by macrophages can inhibit the expression of *SLC7A11* by activating the SMAD-dependent signaling pathway and finally lead to ferroptosis of cancer cells²⁴. Therefore, inhibiting *SLC7A11* may be a promising target for tumour immune therapy.

CFs are part of the cytokine family and play an essential role in the tumour microenvironment. CFs can attract immune cells to enter the tumour microenvironment, thereby affecting the response of the tumour to immunotherapy²⁵. Tumours with fewer CHs may be unresponsive to immune therapy, leading to tumour immune escape.

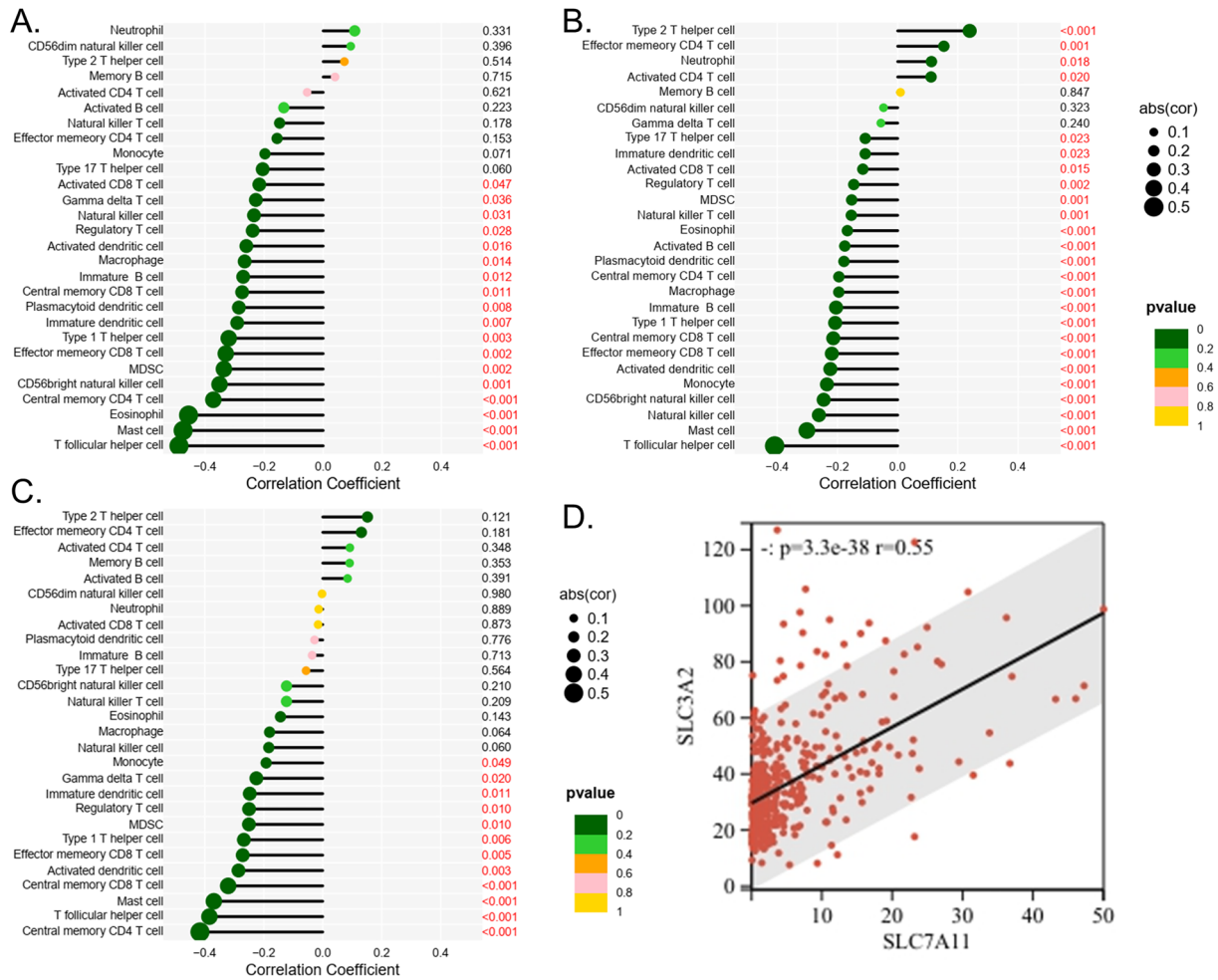


Figure 5. (A) The correlation between *SLC7A11* expression and immune cells in the GSE30219 database. (B) The correlation between *SLC7A11* expression and immune cells in the GSE37745 database. (C) The correlation between *SLC7A11* expression and immune cells in the GSE68465 database. (D) The correlation between *SLC7A11* expression and *SLC3A2* in the TCGA-LUAD database.

This study confirmed that the expression of *SLC7A11* was negatively correlated with the expression of *CCL17/19/22/23*, *CXCL9/10/11/14*, *CCR4/6*, *CX3CR1*, and *CXCR3*, suggesting that high *SLC7A11* expression may inhibit the migration of immune cells. Studies have shown that *CXCL9/10/11* are the main CFs for CD8+ T cells^{26,27,28}, and that *CXCL9/10* can attract Th1 cells to the tumour microenvironment and play an important role against cancer^{28,27}. *CCL17* is the ligand of *CCR4*, and they affect the recruitment of Treg and Th17 cells in tumours²⁹. *CXCR3* and *CX3CR1* are mainly responsible for infiltrating tumour-inhibitory lymphocytes into the tumour microenvironment^{30,31}, further confirming the results of immune cell infiltration. This may explain why patients with high *SLC7A11* expression have poor responses to immunotherapy. The chemokine *CXCL14* is a key regulatory factor in cancer and a potential target for future cancer immunotherapy³². There is also evidence that high *SLC7A11* expression can affect the expression of immune inhibitors and immune stimulators. Therefore, these results suggest that *SLC7A11* may play a role in regulating tumour immunity.

MHCs are a group of highly polymorphic genes, and proteins encoded by MHCs play an important role in the immune system. MHCs are divided into two categories: MHC-I and MHC-II. MHC-I and MHC-II interact with CD8+ T cells and CD4+ T cells respectively, thus activating the immune response^{33,34}. Tumour cells usually express abnormal MHC-I molecules, which allows them to escape attack by CD8+ T cells. In addition, tumour cells can escape immune surveillance by reducing MHC-I expression³⁵. Therefore, restoring MHC-I expression is very important for tumour immunotherapy³⁶. MHC-II can also affect tumour immunity by regulating the activity of immune cells in the tumour microenvironment³⁷.

Previous studies have shown that *SLC7A11* is correlated with *SLC3A2*³⁸. Our study found that the expression of *SLC3A2* was related to *SLC7A11*. In LUAD, we found a lower immune score, matrix score, and ESTIMATE score in the *SLC3A2*-high group, which is consistent with the immune status of the *SLC7A11*-high group. *SLC3A2* is the chaperone protein of *SLC7A11*, which is used to maintain the stability of *SLC7A11* protein and regulate the transport of *SLC7A11* to the plasma membrane. In system Xc-, *SLC7A11* plays a significant role in transport function³⁹.

Chemokines	Rho	p	Chemokines	Rho	p
<i>XCL2</i>	-0.078	0.0753	<i>CCL5</i>	-0.106	0.0162
<i>XCL1</i>	-0.042	0.3410	<i>CCL4</i>	-0.091	0.0386
<i>CXCL9</i>	-0.103	0.0196	<i>CCL3</i>	-0.103	0.0187
<i>CXCL8</i>	0.106	0.0163	<i>CCL28</i>	-0.350	0.0000
<i>CXCL6</i>	-0.060	0.1740	<i>CCL26</i>	0.060	0.1730
<i>CXCL5</i>	0.092	0.0372	<i>CCL24</i>	0.006	0.8860
<i>CXCL3</i>	0.034	0.4380	<i>CCL23</i>	-0.222	0.0000
<i>CXCL2</i>	-0.038	0.3940	<i>CCL22</i>	-0.224	0.0000
<i>CXCL17</i>	-0.124	0.0047	<i>CCL21</i>	-0.014	0.7450
<i>CXCL16</i>	-0.055	0.2090	<i>CCL20</i>	0.172	0.0001
<i>CXCL14</i>	-0.191	0.0000	<i>CCL2</i>	-0.175	0.0001
<i>CXCL13</i>	-0.105	0.0173	<i>CCL19</i>	-0.241	0.0000
<i>CXCL12</i>	-0.191	0.0000	<i>CCL18</i>	-0.040	0.3620
<i>CXCL11</i>	-0.125	0.0045	<i>CCL17</i>	-0.269	0.0000
<i>CXCL10</i>	-0.118	0.0072	<i>CCL15</i>	0.137	0.0018
<i>CXCL1</i>	-0.012	0.7910	<i>CCL14</i>	-0.144	0.0010
<i>CX3CL1</i>	-0.434	0.0000	<i>CCL13</i>	-0.210	0.0000
<i>CCL8</i>	-0.087	0.0471	<i>CCL11</i>	-0.160	0.0003
<i>CCL7</i>	-0.084	0.0577			

Table 3. The correlation between *SLC7A11* expression and CFs.

Receptors	Rho	p	Receptors	Rho	p
<i>CCR1</i>	-0.118	0.0071	<i>CCR10</i>	-0.045	0.3090
<i>CCR2</i>	-0.304	0.0000	<i>CX3CR1</i>	-0.281	0.0000
<i>CCR3</i>	0.151	0.0006	<i>CXCR1</i>	0.137	0.0019
<i>CCR4</i>	-0.253	0.0000	<i>CXCR2</i>	-0.053	0.2250
<i>CCR5</i>	-0.222	0.0000	<i>CXCR3</i>	-0.253	0.0000
<i>CCR6</i>	-0.268	0.0000	<i>CXCR4</i>	-0.184	0.0000
<i>CCR7</i>	-0.236	0.0000	<i>CXCR5</i>	-0.18	0.0000
<i>CCR8</i>	-0.181	0.0000	<i>CXCR6</i>	-0.145	0.0010

Table 4. The correlation between *SLC7A11* expression and chemokine receptor.

Receptors	Rho	p	Receptors	Rho	p
<i>B2M</i>	-0.088	0.0449	<i>HLA-DQA2</i>	-0.301	3.33E-12
<i>HLA-A</i>	-0.098	0.026	<i>HLA-DQB1</i>	-0.343	1.22E-15
<i>HLA-B</i>	-0.224	2.76E-07	<i>HLA-DRA</i>	-0.381	<2.2e-16
<i>HLA-C</i>	-0.144	0.00107	<i>HLA-DRB1</i>	-0.367	1.67E-19
<i>HLA-DMA</i>	-0.356	5.63E-17	<i>HLA-E</i>	-0.208	2.01E-06
<i>HLA-DMB</i>	-0.355	7.47E-17	<i>HLA-F</i>	-0.165	0.000165
<i>HLA-DOA</i>	-0.309	8.83E-13	<i>HLA-G</i>	-0.114	0.00981
<i>HLA-DOB</i>	-0.244	2.05E-08	<i>TPA1</i>	-0.046	0.292
<i>HLA-DPA1</i>	-0.386	<2.2e-16	<i>TPA2</i>	-0.044	0.319
<i>HLA-DPB1</i>	-0.378	<2.2e-16	<i>TAPBP</i>	-0.031	0.483
<i>HLA-DQA1</i>	-0.281	8.76E-11			

Table 5. The correlation between *SLC7A11* expression and chemokine MHCs.

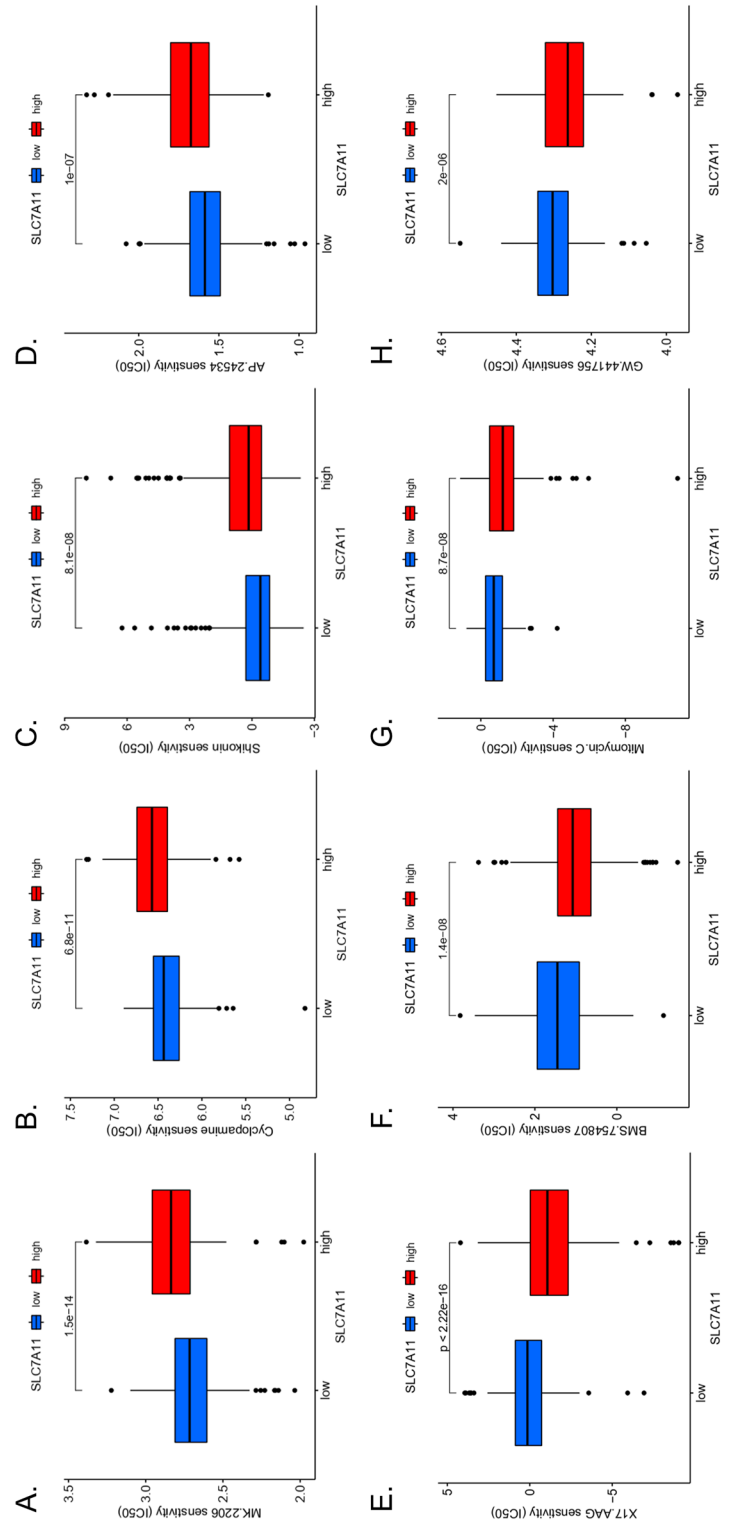


Figure 6. Drug sensitivity analysis. (A)–(D) showed that the drug had a lower IC₅₀ value in the SLC7A11-high group. (E)–(H) showed that the drug had a lower IC₅₀ value in the SLC7A11-low group.

SLC7A11 immune-targeted agents may also be effective adjuvants for chemotherapy. Conti et al. studied the use of combination immunotherapy against HER2 and *SLC7A11*. Antibodies targeting HER2 and *SLC7A11* can inhibit the proliferation and metastasis of BCSCs, exerting synergistic or complementary effects⁴⁰. All of the above suggest that *SLC7A11* may be an important target for treating LUAD, possibly via the regulation of tumour immunity by *SLC7A11*.

Although our research has limitations, it can be considered a verification that we use multiple database sets for analysis. In addition, we used many methods and aspects to verify the relationship between *SLC7A11* and tumor immunity. In order to further verify this exciting discovery, we have been purchasing LUAD cell lines and drugs and collecting clinical specimens of LUAD patients for the next experiment.

Conclusion

In conclusion, this study found that *SLC7A11* was significantly upregulated and may be associated with the prognosis of LUAD. The expression of *SLC7A11* is negatively correlated with the expression of immune checkpoints *PD-L1*, *CTLA4*, and et al. *SLC7A11* is negatively correlated with the expression of many CFs, leading to the loss of immune cells such as CD8+ T cells and causing immune suppression. Regulating the expression of *SLC7A11* may be a potential target for tumor immunotherapy.

Data availability

The TCGA-LUAD dataset was downloaded from the TCGA database (<https://portal.gdc.cancer.gov/>). The GSE30219 dataset was downloaded from the GEO database (<https://www.ncbi.nlm.nih.gov/geo/query/acc.cgi?acc=GSE30219>). The GSE37745 dataset was downloaded from the GEO database (<https://www.ncbi.nlm.nih.gov/geo/query/acc.cgi?acc=GSE37745>). The GSE68465 dataset was downloaded from the GEO database (<https://www.ncbi.nlm.nih.gov/geo/query/acc.cgi?acc=GSE68465>).

Received: 5 July 2023; Accepted: 18 October 2023

Published online: 25 October 2023

References

- Siegel, R. L., Miller, K. D., Wagle, N. S. & Jemal, A. Cancer statistics, 2023. *CA Cancer J. Clin.* **73**, 17–48. <https://doi.org/10.3322/caac.21763> (2023).
- Wang, Z. & Wu, X. Study and analysis of antitumor resistance mechanism of PD1/PD-L1 immune checkpoint blocker. *Cancer Med.* **9**, 8086–8121. <https://doi.org/10.1002/cam4.3410> (2020).
- Lewerenz, J. et al. The cystine/glutamate antiporter system x(c)(-) in health and disease: from molecular mechanisms to novel therapeutic opportunities. *Antioxid. Redox Signal.* **18**, 522–555. <https://doi.org/10.1089/ars.2011.4391> (2013).
- Koppula, P., Zhuang, L. & Gan, B. Cystine transporter SLC7A11/xCT in cancer: ferroptosis, nutrient dependency, and cancer therapy. *Protein Cell* **12**, 599–620. <https://doi.org/10.1007/s13238-020-00789-5> (2021).
- Qian, L. et al. A comprehensive prognostic and immune analysis of ferroptosis-related genes identifies SLC7A11 as a novel prognostic biomarker in lung adenocarcinoma. *J. Immunol. Res.* **2022**, 1951620. <https://doi.org/10.1155/2022/1951620> (2022).
- Ritchie, M. E. et al. limma powers differential expression analyses for RNA-sequencing and microarray studies. *Nucleic Acids Res.* **43**, e47. <https://doi.org/10.1093/nar/gkv007> (2015).
- Joshi, T. & Xu, D. Quantitative assessment of relationship between sequence similarity and function similarity. *BMC Genom.* **8**, 222. <https://doi.org/10.1186/1471-2164-8-222> (2007).
- Kanehisa, M. & Goto, S. KEGG: kyoto encyclopedia of genes and genomes. *Nucleic Acids Res.* **28**, 27–30. <https://doi.org/10.1093/nar/28.1.27> (2000).
- Chen, H. H. et al. GSAE: an autoencoder with embedded gene-set nodes for genomics functional characterization. *BMC Syst. Biol.* **12**, 142. <https://doi.org/10.1186/s12918-018-0642-2> (2018).
- Yoshihara, K. et al. Inferring tumour purity and stromal and immune cell admixture from expression data. *Nat. Commun.* **4**, 2612. <https://doi.org/10.1038/ncomms3612> (2013).
- Geeleher, P., Cox, N. & Huang, R. S. pRRophetic: an R package for prediction of clinical chemotherapeutic response from tumor gene expression levels. *PLoS ONE* **9**, e107468. <https://doi.org/10.1371/journal.pone.0107468> (2014).
- Sun, R., Hou, Z., Zhang, Y. & Jiang, B. Drug resistance mechanisms and progress in the treatment of EGFR-mutated lung adenocarcinoma. *Oncol. Lett.* **24**, 408. <https://doi.org/10.3892/ol.2022.13528> (2022).
- He, J., Ding, H., Li, H., Pan, Z. & Chen, Q. Intra-tumoral expression of SLC7A11 Is associated with immune microenvironment, drug resistance, and prognosis in cancers: a pan-cancer analysis. *Front Genet.* **12**, 770857. <https://doi.org/10.3389/fgene.2021.770857> (2021).
- Tang, B. et al. Macrophage xCT deficiency drives immune activation and boosts responses to immune checkpoint blockade in lung cancer. *Cancer Lett.* **554**, 216021. <https://doi.org/10.1016/j.canlet.2022.216021> (2023).
- Badgley, M. A. et al. Cysteine depletion induces pancreatic tumor ferroptosis in mice. *Science* **368**, 85–89. <https://doi.org/10.1126/science.aaw9872> (2020).
- Qi, D. & Peng, M. Ferroptosis-mediated immune responses in cancer. *Front Immunol.* **14**, 1188365. <https://doi.org/10.3389/fimmu.2023.1188365> (2023).
- Giese, M. A., Hind, L. E. & Huttenlocher, A. Neutrophil plasticity in the tumor microenvironment. *Blood* **133**, 2159–2167. <https://doi.org/10.1182/blood-2018-11-844548> (2019).
- Khalaf, K. et al. Aspects of the tumor microenvironment involved in immune resistance and drug resistance. *Front Immunol.* **12**, 656364. <https://doi.org/10.3389/fimmu.2021.656364> (2021).
- Zhou, Z. et al. Granzyme A from cytotoxic lymphocytes cleaves GSDMB to trigger pyroptosis in target cells. *Science* <https://doi.org/10.1126/science.aaz7548> (2020).
- Yu, X. et al. IFN γ enhances ferroptosis by increasing JAK-STAT pathway activation to suppress SLC7A11 expression in adrenocortical carcinoma. *Oncol. Rep.* <https://doi.org/10.3892/or.2022.8308> (2022).
- Kong, R., Wang, N., Han, W., Bao, W. & Lu, J. IFN γ -mediated repression of system xc(-) drives vulnerability to induced ferroptosis in hepatocellular carcinoma cells. *J. Leukoc Biol.* **110**, 301–314. <https://doi.org/10.1002/jlb.3ma1220-815rrr> (2021).
- Wang, W. et al. CD8(+) T cells regulate tumour ferroptosis during cancer immunotherapy. *Nature* **569**, 270–274. <https://doi.org/10.1038/s41586-019-1170-y> (2019).
- Wei, T. T. et al. Interferon- γ induces retinal pigment epithelial cell ferroptosis by a JAK1-2/STAT1/SLC7A11 signaling pathway in age-related macular degeneration. *FEBS J.* **289**, 1968–1983. <https://doi.org/10.1111/febs.16272> (2022).

24. Kim, D. H., Kim, W. D., Kim, S. K., Moon, D. H. & Lee, S. J. TGF- β 1-mediated repression of SLC7A11 drives vulnerability to GPX4 inhibition in hepatocellular carcinoma cells. *Cell Death Dis.* **11**, 406. <https://doi.org/10.1038/s41419-020-2618-6> (2020).
25. Kanagawa, N. *et al.* CC-chemokine ligand 17 gene therapy induces tumor regression through augmentation of tumor-infiltrating immune cells in a murine model of preexisting CT26 colon carcinoma. *Int. J. Cancer* **121**, 2013–2022. <https://doi.org/10.1002/ijc.22908> (2007).
26. Cheng, C. C. *et al.* Irradiation mediates IFN α and CXCL9 expression in non-small cell lung cancer to stimulate CD8(+) T cells activity and migration toward tumors. *Biomedicines* <https://doi.org/10.3390/biomedicines9101349> (2021).
27. Peperzak, V. *et al.* CD8+ T cells produce the chemokine CXCL10 in response to CD27/CD70 costimulation to promote generation of the CD8+ effector T cell pool. *J. Immunol.* **191**, 3025–3036. <https://doi.org/10.4049/jimmunol.1202222> (2013).
28. Marcovecchio, P. M., Thomas, G. & Salek-Ardakani, S. CXCL9-expressing tumor-associated macrophages: new players in the fight against cancer. *J. Immunother. Cancer* <https://doi.org/10.1136/jitc-2020-002045> (2021).
29. Wenzel, J. *et al.* Role of the chemokine receptor CCR4 and its ligand thymus- and activation-regulated chemokine/CCL17 for lymphocyte recruitment in cutaneous lupus erythematosus. *J. Invest. Dermatol.* **124**, 1241–1248. <https://doi.org/10.1111/j.0022-202X.2005.23755.x> (2005).
30. Groom, J. R. *et al.* CXCR3 chemokine receptor-ligand interactions in the lymph node optimize CD4+ T helper 1 cell differentiation. *Immunity* **37**, 1091–1103. <https://doi.org/10.1016/j.immuni.2012.08.016> (2012).
31. Bronger, H., Magdolen, V., Goettig, P. & Dreyer, T. Proteolytic chemokine cleavage as a regulator of lymphocytic infiltration in solid tumors. *Cancer Metastasis Rev.* **38**, 417–430. <https://doi.org/10.1007/s10555-019-09807-3> (2019).
32. Gowhari Shabgah, A. *et al.* Chemokine CXCL14; a double-edged sword in cancer development. *Int. Immunopharmacol.* **97**, 107681. <https://doi.org/10.1016/j.intimp.2021.107681> (2021).
33. Evans, A. M., Salnikov, M., Tessier, T. M. & Mymryk, J. S. Reduced MHC class I and II expression in HPV-negative vs HPV-positive cervical cancers. *Cells* <https://doi.org/10.3390/cells11233911> (2022).
34. Garrido, F., Ruiz-Cabello, F. & Aptsiauri, N. Rejection versus escape: the tumor MHC dilemma. *Cancer Immunol. Immunother.* **66**, 259–271. <https://doi.org/10.1007/s00262-016-1947-x> (2017).
35. Gu, S. S. *et al.* Therapeutically increasing MHC-I expression potentiates immune checkpoint blockade. *Cancer Discov.* **11**, 1524–1541. <https://doi.org/10.1158/2159-8290.Cd-20-0812> (2021).
36. Dhatchinamoorthy, K., Colbert, J. D. & Rock, K. L. Cancer immune evasion through loss of MHC class I antigen presentation. *Front Immunol.* **12**, 636568. <https://doi.org/10.3389/fimmu.2021.636568> (2021).
37. Griffith, B. D. *et al.* MHC class II expression influences the composition and distribution of immune cells in the metastatic colorectal cancer microenvironment. *Cancers (Basel)* <https://doi.org/10.3390/cancers14174092> (2022).
38. Huang, Y., Dai, Z., Barbacioru, C. & Sadée, W. Cystine-glutamate transporter SLC7A11 in cancer chemosensitivity and chemoresistance. *Cancer Res.* **65**, 7446–7454. <https://doi.org/10.1158/0008-5472.Can-04-4267> (2005).
39. Lin, W. *et al.* SLC7A11/xCT in cancer: biological functions and therapeutic implications. *Am. J. Cancer Res.* **10**, 3106–3126 (2020).
40. Conti, L. *et al.* Immunotargeting of the xCT cystine/glutamate antiporter potentiates the efficacy of HER2-targeted immunotherapies in breast cancer. *Cancer Immunol. Res.* **8**, 1039–1053. <https://doi.org/10.1158/2326-6066.Cir-20-0082> (2020).

Acknowledgements

Script of R language and Perl provided by biowolf_cn (<https://mp.weixin.qq.com/s/kuTGIMFR1bUN63FL4XXXAg>).

Author contributions

Q.S. analyzed and interpreted the data and was a major contributor to writing the manuscript. Y.Z. and X.L. were responsible for statistical data. J.S. and F.H. were responsible for drawing figures. Q.L., C.Z., and Y.L. reviewed the manuscript. All authors read and approved the final manuscript.

Competing interests

The authors declare no competing interests.

Additional information

Supplementary Information The online version contains supplementary material available at <https://doi.org/10.1038/s41598-023-45284-z>.

Correspondence and requests for materials should be addressed to Y.L. or Q.L.

Reprints and permissions information is available at www.nature.com/reprints.

Publisher's note Springer Nature remains neutral with regard to jurisdictional claims in published maps and institutional affiliations.



Open Access This article is licensed under a Creative Commons Attribution 4.0 International License, which permits use, sharing, adaptation, distribution and reproduction in any medium or format, as long as you give appropriate credit to the original author(s) and the source, provide a link to the Creative Commons licence, and indicate if changes were made. The images or other third party material in this article are included in the article's Creative Commons licence, unless indicated otherwise in a credit line to the material. If material is not included in the article's Creative Commons licence and your intended use is not permitted by statutory regulation or exceeds the permitted use, you will need to obtain permission directly from the copyright holder. To view a copy of this licence, visit <http://creativecommons.org/licenses/by/4.0/>.

© The Author(s) 2023